Hindawi Publishing Corporation
Journal of Sensors
Volume 2014, Article ID 145870, 10 pages
http://dx.doi.org/10.1155/2014/145870

Research Article

Denoising Method Based on Sparse Representation for WFT Signal

Xu Chen,[1] Guoyu Lin,[2] and Yuxin Zhang[2]

[1] *School of Information and Control, Nanjing University of Information Science and Technology, Nanjing 210044, China*
[2] *School of Instrument Science and Engineering, Southeast University, Nanjing 210096, China*

Correspondence should be addressed to Xu Chen; sonia.chen@163.com

Received 26 October 2013; Revised 2 January 2014; Accepted 9 January 2014; Published 13 February 2014

Academic Editor: Alexander Vergara

Affected by external noise and various nature disturbances, Wheel Force Transducer (WFT) signal may be completely submerged, and the sensitivity and the reliability of measurement can be strongly decreased. In this paper, a new wavelet packet denoising method based on sparse representation is proposed to remove the noises from WFT signal. In this method, the problem of recovering the noiseless signal is converted into an optimization problem of recovering the sparsity of their wavelet package coefficients, and the wavelet package coefficients of the noiseless signals can be obtained by the augmented Lagrange optimization method. Then the denoised WFT signal can be reconstructed by wavelet packet reconstruction. The experiments on simulation signal and WFT signal show that the proposed denoising method based on sparse representation is more effective for denoising WFT signal than the soft and hard threshold denoising methods.

1. Introduction

Wheel Force Transducer (WFT) can measure the forces and torques (longitudinal force F_x, lateral force F_y, vertical force F_z, heeling moment M_x, twist torque M_y, and aligning torque M_z, which are shown in Figure 1) applied in the wheel dynamically, so it is an important vehicle test device for the research of body vibration, suspension, and wheel dynamics as well as the performance matching of vehicle transmission and braking system [1, 2]. Figure 2 shows the overall structure of WFT which is composed of the elastic body, reforming rims, intermediate flange, sample module, and transfer module. The wheel rims are reformed to connect with the elastic body by bolt, and the intermediate flange is used to protect bridge circuit in the elastic body from water and dirt. The sample module acquires the datum of the wheel's force/torques and rotation angle and then sends them to the transfer module by wireless. Finally the transfer module forwards the datum to the data acquisition devices by CAN bus.

Because the elastic body rotates with the rolling wheel, the outputs of F_x bridge and F_z bridge are similar to sinusoidal signals and the phase difference between them is 90 degree. Figure 3 shows the typical outputs of the two bridges. But all the signals obtained by WFT mounted on wheel are affected by external noise and various nature disturbances when the vehicle is moving. According to the previous research [3, 4], the main causes of these noises include the following (1) Vehicle braking, road roughness and suspension vibration may result in the distortion of WFT signal. (2) As the sensing element, the strain gages are connected to form a Wheatstone bridge. The output of the bridge is only a few millivolts and should be amplified hundreds of times to match the request of data collection. Meanwhile, the electromagnetic noise of the circuit and Johnson noise of the resistance will also be amplified. So even in stationary state the outputs of WFT still fluctuate irregularly. Based on these, the WFT signal is nonstationary signal with random noise which greatly degrades the measurement accuracy of WFT.

In recent years, the wavelet transform has been proposed as an alternative technique that has been applied to the signal processing [5–9]. Wavelet transform involves multiresolution decomposition of the measured data into wavelet coefficients, each having unique time and frequency

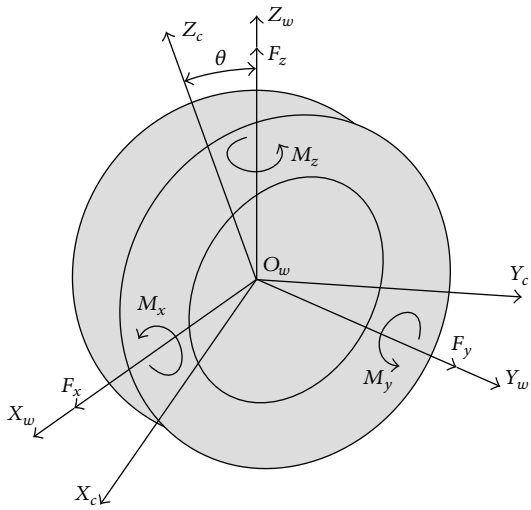

Figure 1: Diagram of forces and torques applied in the wheel.

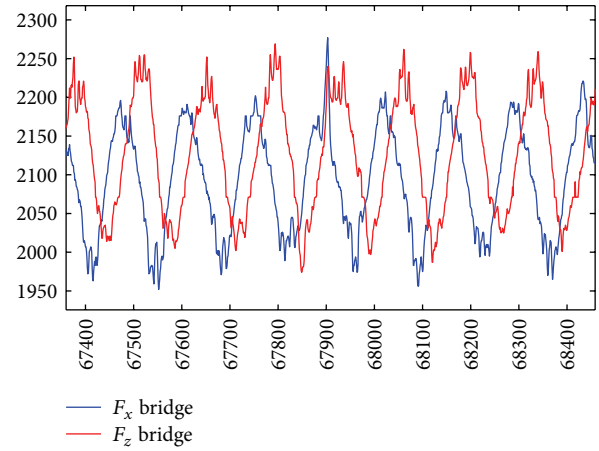

Figure 3: Typical outputs of F_x bridge and F_z bridge.

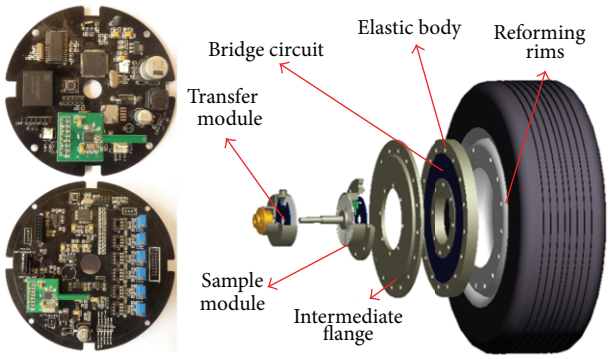

Figure 2: Overall structure of WFT.

information. Compared with Fourier transform, wavelet transform suppresses noises more effectively than Fourier Transform. Due to its merits of low entropy, multiresolution, and decorrelation, wavelet transform (WT) can be used to recover original WFT signal from severe noises [10, 11]. There exist three major forms of wavelet denoising methods. The first method, provided by Mallat and Zhong [12–15], is based on the extrema in the wavelet coefficients which reflect the propagation properties of the signal and noise across wavelet decomposition scales. The second method is called the relativity method [16–21] in which the wavelet coefficients are kept or eliminated according to the magnitude values of their relativities across the neighboring scales. The third method relies on the threshold operation [22, 23] in which the wavelet coefficients whose amplitude values are larger than a given threshold are kept or shrunk while the remaining coefficients are eliminated. Commonly referred to as "hard" or "soft" threshold method, the last one which is the most widely used has the advantages of simplicity and less computer burden. But based on the different distribution of analyzed signal and noises under different resolution and by thresholding empirical wavelet coefficients individually, threshold denoising method ignores the structural properties in the wavelet coefficients [24].

In this paper, based on the compressive sensing theory and sparse theory, a new wavelet packet denoising algorithm with sparse representation (WPDSR) is presented. The proposed algorithm is efficient in recovering the noiseless signal from noisy signal and well suited for WFT signal. The method presented here has two major advantages. First, it employs wavelet packet transform (WPT) for signal decomposition. Similarly to WT, WPT also has the framework of multiresolution analysis. WPT can simultaneously decompose detail and approximation parts of the signal, but WT only decomposes approximation. Therefore, the presented method is more suitable for analyzing signal because of its good resolution regardless of high and low frequencies [25]. Second, sparse representation technique is adopted, aiming at faithfully estimating the noiseless wavelet packet coefficients without losing significant information. It should be noticed that WPDSR is quite different from the denoising method based on sparse decomposition. The latter should construct the over-complete dictionary, based on which the minimum nonzero (most sparse) atoms are solved to reconstruct the noiseless signal. However, WPDSR just selects the sparse and effective wavelet packet coefficients from the original coefficients to reconstruct the noiseless signal without constructing any dictionary.

The rest of the paper is organized as follows. Compared with the hard and soft threshold methods, our proposed method is depicted in Section 2. Then the details of the algorithm are elaborated upon in Section 3 by introducing the sparse representation of the wavelet packet coefficients and showing the denoising framework. In Section 4, to illustrate the efficiency and effectiveness of the proposed denoising method, we review the selection of wavelet base and decomposition level briefly and then report the experimental results on the denoising effectiveness by comparing our proposed methods with hard and soft threshold method. Finally, we draw the conclusions and discuss the future work in Section 5.

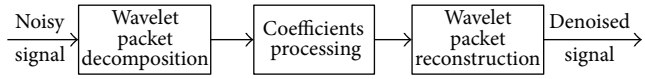

Figure 4: Structure of wavelet packet denoising algorithm with sparse representation.

2. Denoising Principle

Assume that the observed signal is contaminated with additive noise as shown in (1):

$$f(t) = s(t) + n(t), \tag{1}$$

where $f(t)$ and $s(t)$ are the observed and noiseless signals, respectively, and $n(t)$ is a random noise with standard normal distribution $N(0, \sigma^2)$. After wavelet transform, the transformation of (1) to the wavelet domain is

$$f_{jk} = w_{jk} + n_{jk}, \tag{2}$$

where f_{jk}, w_{jk}, and n_{jk} are the wavelet coefficients of observed signal $f(t)$, noiseless signal $s(t)$, and noise signal $n(t)$, respectively, j denotes the decomposition level, and k denotes the index of the coefficient at jth level. From (2), it is clear that the wavelet coefficients of the observed signal can themselves be considered as a noisy version of the wavelet coefficients of the noiseless signal.

Based on the wavelet transform, Donoho proposed the threshold denoising method [21]. The basic of the method is that the coefficients smaller than threshold are considered to be generated by noise and should be set to zero, meanwhile the coefficients larger than threshold are considered to be generated by origin signal and should be remained. Generally, there are soft and hard threshold denoising methods based on the different threshold value quantization, which are defined as follows in (3) and (4), respectively [24]:

$$w_{j,k}^{*} = \begin{cases} \operatorname{sign}\left(w_{jk}\right) \cdot \left(\left|w_{jk}\right| - \lambda\right), & \left|w_{jk}\right| \geq \lambda, \\ 0, & \left|w_{jk}\right| < \lambda, \end{cases} \tag{3}$$

$$w_{j,k}^{*} = \begin{cases} w_{jk}, & \left|w_{jk}\right| \geq \lambda, \\ 0, & \left|w_{jk}\right| < \lambda. \end{cases} \tag{4}$$

In these methods, threshold is usually defined as:

$$\lambda = \sigma \sqrt{\frac{2 \log (N)}{N}}, \tag{5}$$

where $\sigma = \text{median}(|w_{j,k}|)/0.675$ is the noise standard deviation and N is the length of the signal.

In hard threshold method, $w_{j,k}^{*}$ is not continuous, so it brings oscillating to the reconstructed signal; while in soft threshold method, though $w_{j,k}^{*}$ is continuous overall, it has constant deviation with wavelet coefficients and the reconstructed signal appears so smooth that the accuracy comes down to some extent [26]. Moreover, from (3) and (4), it can be seen that in the threshold denoising method, the thresholding process is executed point by point. So the structural property of wavelet coefficients is omitted.

From the principle of the hard and soft threshold methods, the hidden information can be induced as follows.

(1) The wavelet coefficient of noiseless signal is larger than that of noise.

(2) The number of wavelet coefficient of noiseless signal is less than that of observed signal.

From the hidden information and many experiments, we can get an inference that if the wavelet base is selected correctly, the wavelet coefficients of the noiseless signal are sparse. However, if the signal is contaminated by noises, the sparsity of its wavelet coefficients is destroyed [27]. Based on that, we think it is possible to denoise the signal by recovering the sparsity of its wavelet coefficients. And taking the overall structural property of wavelet coefficients into consideration, it will get better denoising performance than hard and soft threshold methods.

3. Wavelet Packet Denoising Algorithm with Sparse Representation

The threshold denoising method uses a coordinate-wise processing scheme, which ignores the structural property of the wavelet coefficients. Instead of thresholding wavelet coefficients individually, we manage a denoising method based on sparse representation according to the compressive sensing theory. The presented denoising algorithm called wavelet packet denoising algorithm with sparse representation (WPDSR) has the following steps (shown in Figure 4).

(1) Wavelet Packet Decomposition. Choose a proper wavelet base function and ascertain the wavelet decomposition level N, and then decompose the signal at N levels by wavelet packet. But there is no unified theory about how to choose wavelet function in the process of denoising. The universal way is to choose and compare the different wavelet functions and find out the best wavelet and its base function.

(2) Coefficients Processing. The key step in WPDSR is the recovery of the noiseless coefficients from the noisy coefficients. We propose to apply sparse representation during this key step. Idealy the wavelet coefficients of noiseless signal should have a small set of large-amplitude values (i.e., sparsity). If the signal is heavily contaminated by noise, the sparsity of the wavelet coefficients decreases [28, 29]. So we approach this problem by employing the powerful sparse

representation technique, aiming at faithfully recovering the sparsity of the wavelet coefficients.

(3) Wavelet Packet Reconstruction. The wavelet packet reconstruction is realized to get the denoised signal based on its resulting coefficients.

Among these three steps, the most important one is how to process the coefficients based on sparse representation. It, to some extent, directly relates to the denoising effectiveness.

3.1. Wavelet Packet Algorithm. The following is the decomposition algorithm of wavelet packet:

$$d_j^{2n}[t] = \sum_{k\in Z} h_{l-2k} d_{j+1}[l], \qquad d_j^{2n+1}[t] = \sum_{k\in Z} g_{l-2k} d_{j+1}[l], \tag{6}$$

where $\{h_k\}$ is the low-pass filter coefficient and $\{g_k\}$ is the high-pass filter coefficient. After passing through a low-pass filter LF and a high-pass filter HF and then being sampled down by a factor of two, the signal can be decomposed into two components, one representing the rapidly time varying features of the signal (output of the HF) and the other representing the slowly time varying features (output of the LF) at a specific scale. These two components are called the detail and the approximation coefficients, respectively. Then the decomposition process is iterated on both the detail and approximate subsequence until the detail and approximate coefficients are suited to the scales for a particular application.

Next is the reconstruction algorithm of wavelet packet:

$$d_{j+1}^{n} = \sum_{k\in Z} h_{k-2l} d_j^{2n}[l] + \sum_{k\in Z} g_{k-2l} d_j^{2n+1}[l]. \tag{7}$$

3.2. Sparse Representation. According to the theory of harmonic analysis, a one-dimensional discrete time signal f whose length is N can be expressed as linear combinations of a set of orthonormal basis $(\psi_i : i = 1, \ldots, m)$ as follows

$$f = \sum_{i=1}^{N} x_i \psi_i, \tag{8}$$

where ψ_i is a column vector and can be, for example, a wavelet basis or a Fourier basis, which depends on the application. $\mathbf{x} = [x_1, x_2, \ldots, x_N]$ is a $N \times 1$ vector which is the weighted coefficients of signal f, and $x_i = \langle f, \psi_i \rangle$. If there are only K nonzero elements in $\mathbf{x}$, then $\mathbf{x}$ can be considered as the K-sparse representation of f.

3.3. Compressive Sensing. Assume that there exists a measurement matrix $\Phi \in R^{M\times N}$ (with M less than N) and a measurement $\mathbf{y}$ which is defined as $\mathbf{y} = \Phi\mathbf{x}$, where $\mathbf{x}$ is an unknown signal. According to compressive sensing theory [30], if $\mathbf{x}$ is K-sparsity, then the unknown signal $\mathbf{x}$ can be recovered by solving the following equation:

$$\widehat{x} = \arg\min \|x\|_0 \quad \text{s.t. } y = \Phi x, \tag{9}$$

where $\|\cdot\|_0$ is L_0 norm which means the number of the nonzero elements in $\mathbf{x}$.

3.4. WPDSR

3.4.1. Denoising Mode. The theories of sparse representation and compressive sensing can be applied to the signal denoising. For wavelet basis is a kind of orthonormal basis, if the signal is noiseless, according to Section 3.2 the wavelet coefficients of the signal is K-sparsity. However according to Section 2, if the signal is contaminated by noise, the sparsity of their wavelet coefficients will decrease. This means that the nonzero elements of wavelet coefficients will be beyond K. Suppose s and f represent the noiseless signal and noisy signal and their elements satisfy (1) or (2). Let w^* denote the wavelet packet coefficients of s and w denote the wavelet packet coefficients of f. According to Section 2, if we can recover w^* from w, then we can recover the noiseless signal s from the noisy signal f.

According to Section 3.3, because w^* is sparse but unknown and w can be obtained by WPT, then if we can find a suitable measurement matrix Φ, then w^* can be solved by the following equation:

$$\widehat{w}^* = \arg\min \|w^*\|_0 \quad \text{s.t. } w = \Phi w^*. \tag{10}$$

Considering the reconstruction error, (10) can be converted to (11) by replacing the equality constraints with inequality constraints:

$$\widehat{w}^* = \arg\min \|w^*\|_0 \quad \text{s.t. } \|w - \Phi w^*\| \le \varepsilon, \tag{11}$$

where ε is the error tolerance.

It should be noticed that one of the preconditions of (9) or (10) is that the measurement matrix Φ should satisfy the restricted isometry constants. Being independent of any orthonormal basis approximately [31, 32], Gaussian random matrix satisfies the restricted isometry constants and can be exploited as the measurement matrix Φ.

So it is clear that the problem of recovering the noiseless signals is converted to an optimization problem of recovering the sparsity of their wavelet packet coefficients. If the optimal solution is acquired, the noise can be removed from the signal.

3.4.2. Solution of the Denoising Model. The equation shown in (11) cannot be solved in general because it is an NP-hard problem in combinatorial mathematics. Here we apply augmented Lagrange multiplier method to handle the problem with inequality constraint in order to avoid the ill condition of the augmented Lagrange function and the dependency of the penalty parameters of the traditional penalty function. The augmented Lagrange function for this constrained optimization problem shown in (11) can be defined as follows [33]:

$$L_\alpha(w^*, \beta, \gamma) = \|w\|_0 + \gamma\left[\max\left(\|w - \phi w^*\|_2 - \varepsilon, -\frac{\beta}{2\gamma}\right)\right]^2 + \beta\left[\max\left(\|w - \phi w^*\|_2 - \varepsilon, -\frac{\beta}{2\gamma}\right)\right], \tag{12}$$

where γ is a penalty parameter and the corresponding Lagrange multiplier β is associated with inequality constraint.

(1) choose the proper wavelet basic;
(2) calculate $w^j (j = 1, \ldots, J)$ using WPD;
(3) let $j = J$;
(4) while $j <> 1$
  (1) let $w_0^j = 0$ and $w_1^j = \beta^j$;
  (2) while $\left\| w_1^j - w_0^j \right\| > \varepsilon$ do
    $w_0^j = w_1^j$;
    compute w_1^j by (12);
  (3) let $w^{*j} = w_1^j$;
  (4) $j = j - 1$;
(5) reconstruct the signal by w^{*j};

Algorithm 1: Flowchart of the proposed denoising algorithm.

To solve this constrained optimization problem, the iterative algorithm is adopted. In each iteration, the Lagrange multiplier β and the penalty parameter γ are updated in order to improve the convergence of the algorithm. The Lagrange multiplier β is typically updated as follows:

$$\beta^{j+1} = \beta^j + 2\gamma \left[\max \left(\left\| w - \phi w^* \right\|_2 - \varepsilon, -\frac{\beta}{2\gamma} \right) \right]. \quad (13)$$

And the penalty parameter γ is increased by a constant rate until it reaches the predetermined maximum value $\gamma_{\max}$ as shown below:

$$\gamma^{j+1} = \begin{cases} c \times \gamma^j, & \text{if } \gamma^j < \gamma_{\max}, \\ \gamma_{\max}, & \text{otherwise}, \end{cases} \quad (14)$$

where c is the positive constant increasing rate and $\gamma_{\max}$ is the maximum penalty multiplier corresponded with inequality constraint.

3.4.3. Denoising Steps. The wavelet packet coefficients of the noiseless signal are correlated across levels, so it is likely that the nonzero wavelet packet coefficients are located in the similar area at different levels. Therefore, the wavelet packet coefficients at the jth level can be predicted from the coefficients at the $(j + 1)$th level, which helps to select the initial value iteratively at each level. Based on it, the detailed steps of the proposed denoising algorithm based on sparse representation are listed in Algorithm 1, and some priori knowledge and symbol are given below:

(1) J is the wavelet packet decomposition level;

(2) w^j $(j = 1, \ldots, J)$ is the wavelet packet coefficients of noisy signal at jth level;

(3) w^{*j} $(j = 1, \ldots, J)$ is the reconstructed wavelet packet coefficients at jth level;

(4) Φ is the measurement matrix; as shown in Section 3.4.1 Gaussian random matrix is used;

(5) β^j $(j = 1, \ldots, J)$ is the iterative initial value at jth level; according to the correlation of wavelet packet coefficients across levels shown above, β^j is set as

$$\beta^j = \begin{cases} w^J, & \text{if } j = J, \\ w^{*j+1}, & \text{if } j < J. \end{cases} \quad (15)$$

4. Experiments and Results

To verify the effectiveness of the presented method, the simulation WFT signal and real WFT signal are exploited, and SNR (signal-to-noise ratio) and CC (correlation coefficient) are used to evaluate the denoising performance, which are formulated as follows [34]:

$$\text{SNR (db)} = 10 \times \log_{10} \frac{\text{Energy (signal)}}{\text{Energy (noise)}},$$
$$\text{CC} = \frac{\sum_{i=1}^{N} \left(F(i) - \overline{F} \right) \left(R(i) - \overline{R} \right)}{\sqrt{\sum_{i=1}^{N} \left(F(i) - \overline{F} \right)^2} \sqrt{\sum_{i=1}^{N} \left(R(i) - \overline{R} \right)^2}}, \quad (16)$$

where F and R are the denoised and noise-free signals, respectively, $\overline{F}$ and $\overline{R}$ are the mean value of F and R, respectively, and N is the length of the signal F.

SNR measures the ratio between the energy of signal and that of noise, and the smaller the SNR is, the better the denoising effect is. CC measures the similarity between the denoised signal and the noise-free signal, so the larger the CC is, the more similar they are and the better the performance is.

Because the outputs of F_x bridge and F_z bridge of WFT are similar to the sinusoidal signals with random noise, we select them as the simulation signal, and the frequency is 50 Hz, 55 Hz, 60 Hz, 65 Hz, and 70 Hz, respectively, with different SNR.

4.1. Selection of Wavelet and Decomposition Level. The selection of an optimal wavelet and the decomposition level is two important issues of the wavelet packet decomposition.

The first task to be accomplished is to choose the optimal wavelet. In this paper, a method based on minimum prominent decomposition coefficients [35] is extended to choose the optimal wavelet from a set of wavelet bases candidates including Daubechies, Symlets, and Coiflets, considering the features such as regularity and vanishing moments. For each candidate wavelet, the method first decomposes the signal into the wavelet packet domain down to a predetermined level of 4. Secondly, the average of absolute values (denoted as η) of detail wavelet packet coefficients is calculated for each decomposition level and then summated across all decomposition levels, and it is formulated as $\eta = \sum_{j=1}^{J} \text{abs}(d_j^{2n})/N_j$, where j $(j = 1, \ldots, J)$ is the decomposition level and d_j^{2n} is the nth $(n = 1, \ldots, N_j)$ detail coefficient at jth level. η indicates how closely the candidate wavelet is describing the selected signal, and the smaller η is, the better the performance is. Then this procedure is applied to all signals by all candidates wavelets. The wavelet giving the lowest η is chosen as the best

Table 1: η of test signals with 5 dB SNR by different wavelet.

Wavelet	Frequency (Hz)				
	50	55	60	65	70
db2	1.4931	1.5620	1.5549	1.5129	1.4843
db4	1.1897	1.2464	1.2392	1.1830	1.1897
db6	1.0958	1.1454	1.1058	1.0634	**1.0950**
db8	1.0840	1.1089	**1.0548**	**1.0112**	**1.0716**
db10	**1.0375**	**1.0904**	**1.0633**	**0.9943**	**1.0374**
sym2	1.4931	1.5620	1.5549	1.5129	1.4843
sym4	1.1938	1.2521	1.2455	1.1881	1.1904
sym6	1.0991	1.1534	1.1357	1.0785	1.1159
sym8	**1.0558**	**1.0788**	**1.0553**	1.0394	1.1072
sym10	**1.0229**	**1.0896**	1.0634	**1.0364**	1.1336
coif2	1.2084	1.2639	1.2353	1.1895	1.2048
coif3	1.1405	1.2096	1.1836	1.1142	1.1283
coif4	1.1243	1.1508	1.1498	1.1009	1.1614
coif5	1.1372	1.1499	1.0808	1.0635	1.1697

wavelet. Table 1 shows the results of the simulation signal with 5 dB SNR, and the three smallest η are displayed in bold. From Table 1, it can be seen that wavelet "db10" could achieve the best performance because of the lower η. The similar results are obtained for other signals with different SNR, which are not listed here in detail for lack of space forbids. So "db10" is chosen as the wavelet for WFT signal decomposition.

Besides the optimal choice of the wavelet, how to select the best decomposition level is also important. In the above experiments the decomposition level is preset ($J = 4$). To asses the performance of the wavelet at other decomposition levels, all the parameters above are kept unchanged except the decomposition level, then we can see how the decomposition level influences the denoising effect of the proposed method. Figures 5 and 6 show the influence of decomposition level on SNR and CC for the simulation signal with 5 dB SNR, from which it can be seen that SNR and CC could hardly increase when the decomposition level gets beyond 5. The similar results are obtained for signals with different SNR. As we know the less the wavelet decomposition level is, the less the computational operation of signal denoising will be. So according to the experimental results, we choose the optimal decomposition scale ($J = 5$) during the following denoising experiments.

4.2. Comparison of Different Denoising Methods for Simulation Signal. To evaluate the denoising performance of WPDSR, our proposed method is compared with the threshold method including soft and hard. In the experiments, the parameters of the proposed WPDSR are set empirically:

(1) the error tolerance ε is set as 1;

(2) the maximum penalty multiplier $\gamma_{\max}$ is set as 10;

(3) the positive constant c is set as 0.1.

Table 2 shows SNR and CC of the denoised signal by the different denoising methods. From Table 2, it can be seen that the presented denoising method leads to the largest SNR and

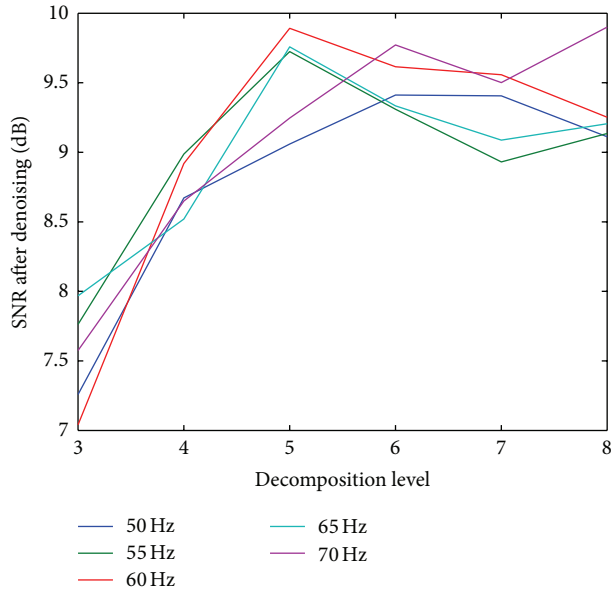

Figure 5: Influence of decomposition level on SNR.

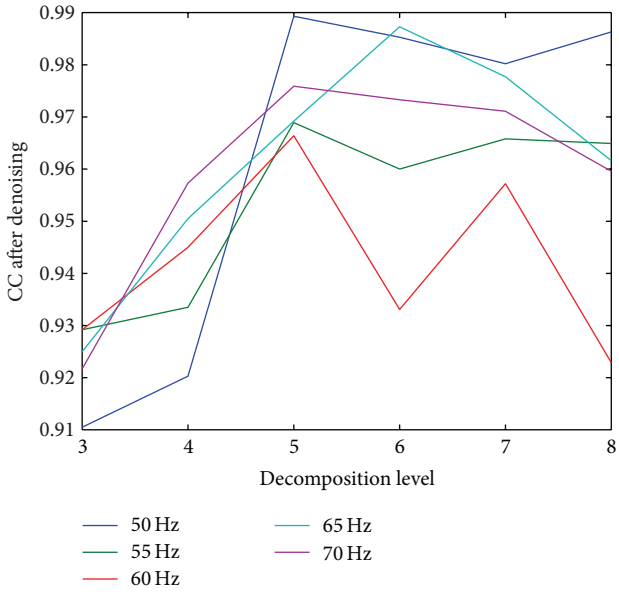

Figure 6: Influence of decomposition level on CC.

CC after denoising. This means that WPDSR outperforms the other two methods for both noise reduction and signal restoration.

As an example, the denoising results of the simulation noisy signal with SNR = 5 dB and frequency = 50 Hz using the proposed method as well as the other mentioned methods are shown in Figure 7. It is obvious that the curve denoised by the proposed method is much smoother than the curve denoised by the other two methods. And the mean of squared error (MSE) from hard threshold, soft threshold, and our method are 0.5376, 0.4880, and 0.4184, respectively, so the absolute

Table 2: Comparison of SNR and CC by using the three different denoising methods.

SNR before denoising	Frequency	SNR after denoising (dB)			CC after denoising		
		Hard threshold	Soft threshold	The proposed method	Hard threshold	Soft threshold	The proposed method
10 dB	50	11.8975	12.5750	13.3241	0.9901	0.9908	0.9912
	55	12.1520	12.8504	13.4851	0.9798	0.9813	0.9845
	60	11.7591	12.4382	13.5607	0.9732	0.9735	0.9756
	65	11.6483	12.0538	13.2084	0.9789	0.9800	0.9812
	70	11.5608	12.4672	13.6375	0.9816	0.9833	0.9863
5 dB	50	8.0593	8.8428	9.0593	0.9843	0.9854	0.9893
	55	8.3879	8.8534	9.7245	0.9620	0.9632	0.9689
	60	8.3189	9.0547	9.8915	0.9609	0.9637	0.9664
	65	8.0125	8.8504	9.7581	0.9636	0.9658	0.9692
	70	7.5483	8.1592	9.2461	0.9709	0.9724	0.9759
0 dB	50	6.1360	6.8254	7.5268	0.9738	0.9755	0.9780
	55	5.8967	6.5249	7.0423	0.9586	0.9614	0.9631
	60	5.1586	5.4860	6.7808	0.9694	0.9721	0.9743
	65	6.1404	6.5328	7.0524	0.9638	0.9645	0.9672
	70	5.1453	5.8918	6.9245	0.9652	0.9674	0.9695
−5 dB	50	3.5524	3.9805	4.5246	0.9631	0.9647	0.9663
	55	2.8593	3.4395	4.1250	0.9646	0.9651	0.9684
	60	2.7695	3.0256	3.8925	0.9659	0.9683	0.9705
	65	3.1369	3.5284	4.2386	0.9571	0.9588	0.9594
	70	3.1245	3.8925	4.8425	0.9609	0.9613	0.9635
−10 dB	50	1.2534	1.8562	2.5851	0.9476	0.9489	0.9498
	55	1.5962	2.1256	2.8408	0.9549	0.9553	0.9563
	60	1.2564	1.7592	2.3614	0.9423	0.9428	0.9446
	65	0.9547	1.5410	2.0596	0.9362	0.9365	0.9372
	70	1.5814	1.9854	2.5468	0.9438	0.9443	0.9456

error from the proposed method is much smaller than that from the other two methods.

4.3. Comparison of Different Denoising Methods for WFT Signal. To verify the effectiveness of the proposed method in the real application, the real WFT signal is denoised by the above methods. Figure 8 shows the denoising results of the F_x bridge output by the proposed method, soft threshold method, and hard threshold method. It can be seen that the WPDSR obtains superior visual quality.

To further show the performance of the proposed method acting on the WFT signal processing, we use the original and the denoised bridge outputs to obtain the longitudinal force F_x and twist torque M_y applied to the wheel. Figure 9 shows the comparison of the original and the denoised force/torque in an acceleration course. There exist two gear shifts in this experiment. During shifting T1-T2 the driver presses the clutch, and then the engine and the gearbox detach. Then the driver presses the accelerator pedal in T2-T3. After that shifting T3-T4 follows. In this acceleration process the output torque of the gearbox causes F_x and M_y to change correspondingly.

From Figures 8 and 9, it is shown that the proposed denoising method can effectively remove the noise from the output of WFT and the force/torque applied to the wheel can be measured effectively by using the proposed method.

5. Conclusions

Although the standard wavelet threshold denoising method is simple and practical, it does not work well for signals with a low SNR; besides, it uses coordinate-wise processing without taking the structural information of the wavelet coefficients into account. In this paper, the new denoising method based on wavelet packet transform and sparse representation is used to overcome these problems. It can estimate the noise-free wavelet packet coefficients by solving an optimization problem and is suitable for signals with a low SNR. Experiments were conducted on different simulation signals, which were corrupted by various noise levels, to assess the performance of the proposed algorithm in comparison with soft and hard threshold denoising methods. The analysis of the results indicated that the proposed method outperforms the universal hard threshold and soft threshold methods and

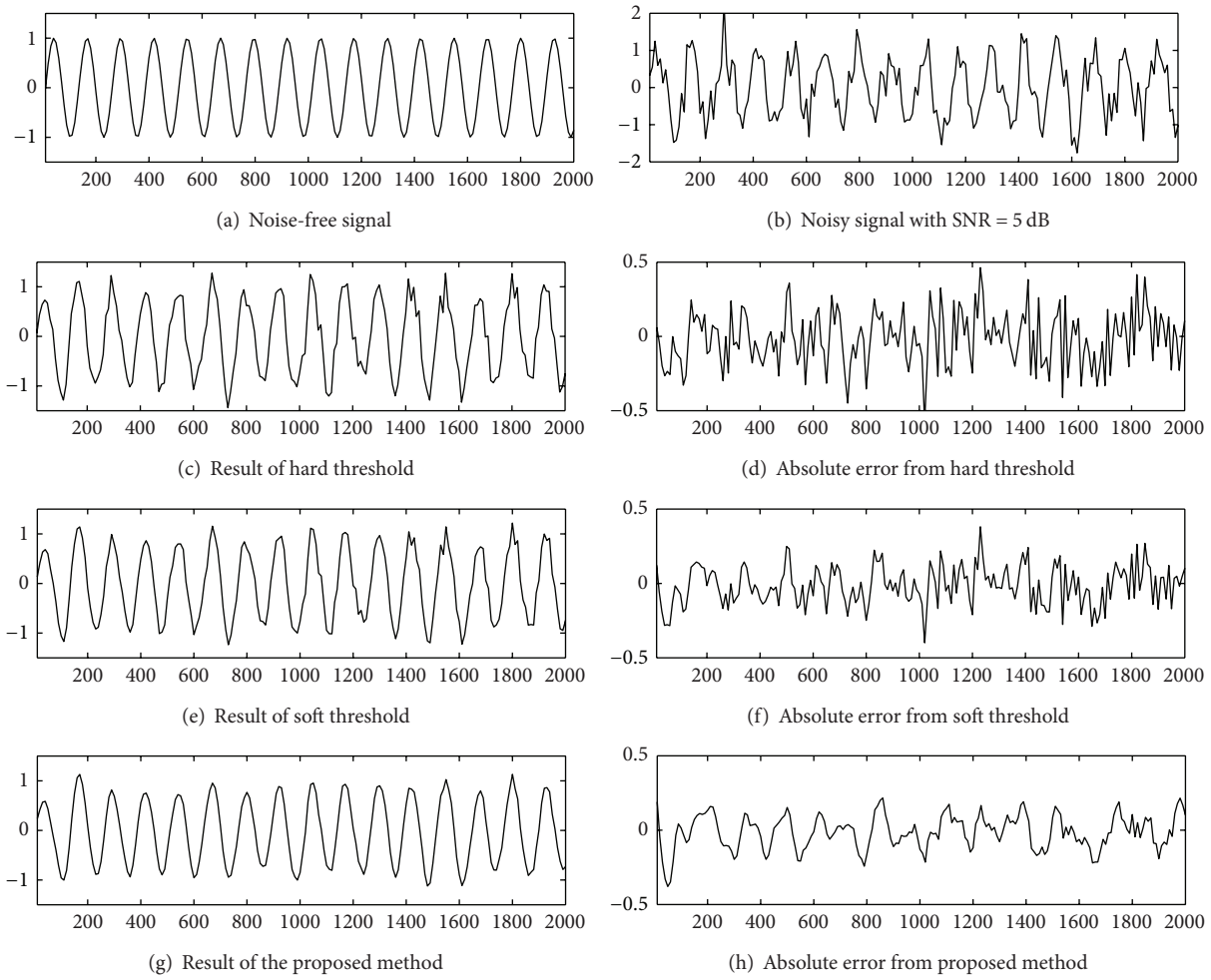

Figure 7: Comparison of the denoising performance for simulation WFT signal with SNR = 5 dB.

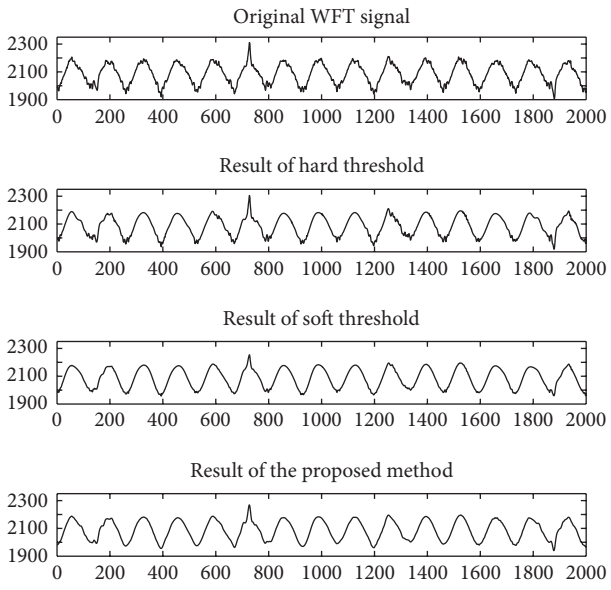

Figure 8: Comparison of the denoising performance for real WFT signal.

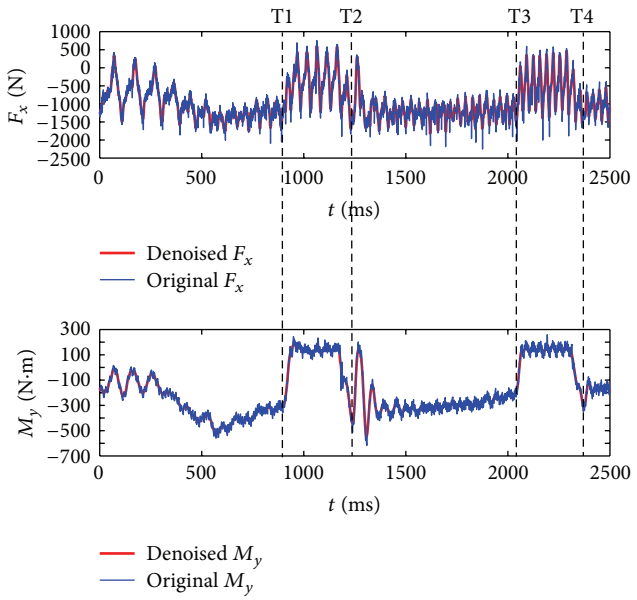

Figure 9: F_x and M_y in an acceleration process.

it could be competent for denoising WFT signal with heavy noise. Through the relevant graphs and data, the superiority of the presented method is illustrated clearly. Furthermore, the proposed method also can be used in other applications and should acquire satisfactory results.

Conflict of Interests

The authors declare that there is no conflict of interests regarding the publication of this paper.

Acknowledgments

This work was supported by the National Natural Science Foundation of China (nos. 51305078 and 61272223).

References

[1] X. Zhang, N. Feng, and W. Zhang, "Experimental research on the abs performance based on the wheel forces measured by roadway test," *China Mechanical Engineering*, vol. 19, no. 6, pp. 751–755, 2008.

[2] M. Corno, M. Gerard, M. Verhaegen, and E. Holweg, "Hybrid ABS Control Using Force Measurement," *IEEE Transactions on Control Systems Technology*, vol. 20, no. 5, pp. 1223–1235, 2011.

[3] W. G. Zhang, "Study on multi-component wheel force measurement technology," *Journal of Jiangsu University*, vol. 25, no. 1, pp. 25–28, 2004.

[4] G. F. Liu, W. G. Zhang, and Z. G. Li, "Research on static decoupling for multi dimensional wheel force transducer," *Instrument Technique and Sensor*, vol. 7, pp. 15–18, 2006.

[5] A. Grinsted, J. C. Moore, and S. Jevrejeva, "Application of the cross wavelet transform and wavelet coherence to geophysical times series," *Nonlinear Processes in Geophysics*, vol. 11, no. 5-6, pp. 561–566, 2004.

[6] M. Antonini, M. Barlaud, P. Mathieu, and I. Daubechies, "Image coding using wavelet transform," *IEEE Transactions of Image Processing*, vol. 1, no. 2, pp. 205–220, 1992.

[7] E. Matsuyama, D.-Y. Tsai, Y. Lee et al., "Comparison of a discrete wavelet transform method and a modified undecimated discrete wavelet transform method for denoising of mammograms," in *Proceedings of the 35th Annual International Conference of the IEEEEngineering in Medicine and Biology Society (EMBC '13)*, pp. 3403–3406, 2013.

[8] J. S. Murgui'a, A. Vergaraa, C. Vargas-Olmos et al., "Two-dimensional wavelet transform feature extraction for porous silicon chemical sensors," *Analytica Chimica Acta*, vol. 785, pp. 1–15, 2013.

[9] P. Ghorbanian, D. M. Devilbiss, A. Verma et al., "Identification of resting and active state EEG features of Alzheimer's disease using discrete wavelet transform," *Annals of Biomedical Engineering*, vol. 41, no. 6, pp. 1243–1257, 2013.

[10] Q. Liu and W. Zhang, "Design of acquisition system for road loading spectra data based on wheel force transducer," *Journal of Jiangsu University*, vol. 32, no. 4, pp. 389–393, 2011.

[11] G. F. Liu, W. D. Zhu, W. G. Zhang, and S. G. Li, "De-noising of signals of wheel force transducer based on wavelet transform," *Instrument Technique and Sensor*, vol. 1, pp. 44–46, 2007.

[12] S. Mallat and S. Zhong, "Characterization of signals from multiscale edges," *IEEE Transactions on Pattern Analysis and Machine*, vol. 14, no. 7, pp. 710–732, 1992.

[13] C. Bai, Y. Peng, and Q. Zhang, "A new wavelet transform modulus maximum denoising algorithm for UWB system," *Advanced Materials Research*, vol. 443-444, pp. 542–547, 2012.

[14] Z. Fan, M. Cai, and H. Wang, "An improved denoising algorithm based on wavelet transform modulus maxima for non-intrusive measurement signals," *Measurement Science and Technology*, vol. 23, no. 4, Article ID 045007, pp. 1–11, 2012.

[15] Y. Qin, J. Wang, and Y. Mao, "Signal denoising based on soft thresholding and reconstruction from dyadic wavelet transform modulus maxima," *Journal of Vibration, Measurement and Diagnosis*, vol. 31, no. 5, pp. 543–547, 2011.

[16] Y. Xu, J. B. Weaver, D. M. Healy Jr., and J. Lu, "Wavelet transform domain filters: a spatially selective noise filtration technique," *IEEE Transactions on Image Processing*, vol. 3, no. 6, pp. 747–758, 1994.

[17] W. Zhan, J. Tan, and Y. Wen, "Denoising algorithm based on correlation of inter scales wavelet coefficient for damage signal of wire rope," *Advanced Materials Research*, vol. 328–330, pp. 2027–2031, 2011.

[18] Q. Xiao, J.-H. Wang, X.-K. Fang, and S.-P. Guan, "A wavelet coefficient threshold denoising method based on a cross-correlation function," *Journal of Northeastern University*, vol. 32, no. 3, pp. 318–321, 2011.

[19] Z.-G. Zhang, X.-J. Zhou, F.-C. Yang, and M.-X. Xie, "Denoising method based on wavelet transform coefficient correlation and local laplacian model," *Journal of Vibration and Shock*, vol. 27, no. 11, pp. 32–36, 2008.

[20] J. Portilla and E. P. Simoncelli, "Image denoising via adjustment of wavelet coefficient magnitude correlation," in *Proceedings of the International Conference on Image Processing (ICIP '00)*, pp. 277–280, September 2000.

[21] D. L. Donoho, "De-noising by soft-thresholding," *IEEE Transactions on Information Theory*, vol. 41, no. 3, pp. 613–627, 1995.

[22] J. Hairong, R. Yongmei, and Z. Xueying, "An improved wavelet packet threshold function for speech enhancement method," *Journal of Information and Computational Science*, vol. 10, no. 3, pp. 941–948, 2013.

[23] Z. Di, J. Zhang, and C. Jia, "An improved wavelet threshold denoising algorithm," in *Proceedings of the 3rd International Conference on Intelligent System Design and Engineering Applications (ISDEA '13)*, pp. 297–299, 2013.

[24] X. Dong, Y. Yue, X. Qin, X. Wang, and Z. Tao, "Signal denoising based on improved wavelet packet thresholding function," in *Proceedings of the International Conference on Computer, Mechatronics, Control and Electronic Engineering (CMCE '10)*, pp. 382–385, August 2010.

[25] I. Daubechies, "Wavelet transform, time-frequency localization and signal analysis," *IEEE Transactions on Information Theory*, vol. 36, no. 5, pp. 961–1005, 1990.

[26] Z. Yongxiang, Z. Xiaoxu, Y. Huimei, and Z. Weigong, "Wavelet packet threshold approach to denoising piezoelectricity gyro signal," in *Proceedings of the International Conference on Computer Engineering and Technology*, pp. 266–269, Singapore, 2009.

[27] R. Zhao, X. Liu, C.-C. Li, R. J. Sclabassi, and M. Sun, "A new denoising method based on Wavelet transform and sparse representation," in *Proceedings of the 9th International Conference on Signal Processing (ICSP '08)*, pp. 171–174, Beijing, China, October 2008.

[28] D. L. Donoho, "Compressed sensing," *IEEE Transactions on Information Theory*, vol. 52, no. 4, pp. 1289–1306, 2006.

[29] R. G. Baraniuk, "Compressive sensing," *IEEE Signal Processing Magazine*, vol. 24, no. 4, pp. 118–124, 2007.

[30] S.-T. Li and D. Wei, "A survey on compressive sensing," *Acta Automatica Sinica*, vol. 35, no. 11, pp. 1369–1377, 2009.

[31] E. J. Candès, J. K. Romberg, and T. Tao, "Stable signal recovery from incomplete and inaccurate measurements," *Communications on Pure and Applied Mathematics*, vol. 59, no. 8, pp. 1207–1223, 2006.

[32] E. J. Candes and T. Tao, "Decoding by linear programming," *IEEE Transactions on Information Theory*, vol. 51, no. 12, pp. 4203–4215, 2005.

[33] G. Yan, H. Wang, G. Ding, and L. Lin, "Augmented Lagrange multiplier based fuzzy evolutionary algorithm and application for constrained optimization," in *Proceedings of the 4th World Congress on Intelligent Control and Automation*, pp. 1774–1778, June 2002.

[34] C. Petrarca and G. Lupò, "Wavelet packet denoising of partial discharge data," in *Proceedings of the Conference on Electrical Insulation and Dielectric Phenomena (CEIDP '06)*, pp. 644–647, October 2006.

[35] C. S. Chang, S. Kumar, Q. Su et al., "Denoising of partial discharge signals in wavelet packets domain," *IEEE Proceedings: Science, Measurement and Technology*, vol. 152, no. 3, pp. 129–140, 2005.